 https://doi.org/10.3311/PPci.23815

Periodica Polytechnica Civil Engineering, 68(4), pp. 1314–1327, 2024

Investigation on NSM-CFRP Ropes Shear Strengthened RC Beams with an Inclusion of Steel-reinforced Geopolymer in the Compressive Zone

Gathot Heri Sudibyo[1,2*], Sri Tudjono[2], Ilham Nurhuda[2]

[1] Department of Civil Engineering, Faculty of Engineering, Jenderal Soedirman University, Jln. Mayjen. Sungkono KM 5, Blater, 53371 Purbalingga, Indonesia
[2] Department of Civil Engineering, Faculty of Engineering, Diponegoro University, Jln. Prof. Soedarto, Tembalang, 50375 Semarang, Indonesia
* Corresponding author, e-mail: gathot.sudibyo@unsoed.ac.id

Received: 09 November 2023, Accepted: 04 June 2024, Published online: 11 July 2024

Abstract

The field of structural engineering was focused on the growth of the latest technologies, materials, and techniques that promoted sustainability, and the use of Carbon Fiber Reinforced Polymer (CFRP) as well as geopolymer was a prime example of this effort. Several investigations and developments in composite materials have generated a wide range of materials that could be used to enhance the strength and durability of structures. This study introduces a novel approach to shear strengthening of reinforced concrete (RC) beams by utilizing Near Surface Mounted (NSM) CFRP ropes in combination with steel-reinforced geopolymer in the compressive zone. The investigation aims to assess the effectiveness of these advanced composite materials in enhancing the structural performance of RC beams, as opposed to conventional steel rebar. Three specimens were subjected to three-point bending tests, demonstrating that the NSM-CFRP ropes, paired with steel-reinforced geopolymer, significantly increased load-carrying capacity. Additionally, the results indicated substantial improvements in ductility and energy absorption. This research contributes to the field by providing a sustainable and efficient alternative to traditional strengthening techniques, supported by a comprehensive assessment of both experimental and numerical findings.

Keywords

beam, flexure, shear, strengthening, CFRP

1 Introduction

According to preliminary studies, structural defects are commonly found in existing buildings during assessments and inspections, particularly in older constructions that do not meet current design standards [1–4]. Although strength was traditionally prioritized in structural design, ductility is now recognized worldwide as essential for structural performance against earthquakes, as reflected in seismic design provisions and standards [5]. Earthquakes in Indonesia have caused widespread damage over the past few decades, highlighting the need to reduce the vulnerability of buildings to seismic activity [6]. Therefore, it is essential to work on the development of methods that are both effective and economical for the purpose of strengthening and rehabilitating structures.

Continuous investigation and development of strengthening methods are crucial for maintaining and potentially increasing the structural arrangement of existing buildings while also providing better environments for occupants [7–10]. One traditional rehabilitation method for reinforced concrete (RC) beams with poor detailing or damage involves applying steel or concrete jackets around the structural components [11–13]. However, such methods increase the dead load and pose the risk of corrosion development in the case of steel jackets.

In modern times, it is recommended to use environmentally friendly materials for repairing RC structures, and many research projects investigated the use of these materials [14–16]. The bond behavior of these materials is found to be satisfactory, enhancing the strength and durability of the repaired RC elements. In order for RC elements to be repaired effectively, it is crucial that the applied materials are compatible with the concrete substance in terms of bonding [17]. Ahmad Zailani et al. [18] previously studied

Cite this article as: Sudibyo, G. H., Tudjono, S., Nurhuda, I. "Investigation on NSM-CFRP Ropes Shear Strengthened RC Beams with an Inclusion of Steel-reinforced Geopolymer in the Compressive Zone", Periodica Polytechnica Civil Engineering, 68(4), pp. 1314–1327, 2024. https://doi.org/10.3311/PPci.23815

the bond strength between a geopolymer matrix composed of fly ash and a concrete surface. The findings revealed that the repair material had a higher density and fewer pores. Additionally, the researchers discovered that the mechanical and bond strength can be improved by using a geopolymer with high calcium content.

Geopolymer is an innovative and sustainable cementitious material that has generated significant interest in the building industry. It is created through polymerization, an exothermic process that combines naturally available silica (SiO) with alumina (Al_2O_3) in an alkaline solution to create an amorphous material with exceptional structural strength. An alkaline component activates the process, and polymerization occurs under alkaline conditions to create polymeric SiO-Al-O bonds. Due to its excellent workability, chemical compatibility, and thixotropic performance, geopolymer has been identified as a useful material for rehabilitation purposes [19]. Pacheco-Torgal et al. [20] have provided a review of the possible applications of geopolymers for concrete structures rehabilitation.

Meanwhile, in recent decades, the materials of fiber-reinforced polymer (FRP) have made significant progress in the field of structural strengthening and rehabilitation. FRP composites are now considered a practical alternative to conventional techniques because they can be used with various materials such as concrete [21–29], steel [30, 31], wood [32, 33], and masonry [34, 35], to enhance the structural elements' performance. These composites are created by combining diverse materials to improve their capabilities and overcome their limits. The reinforcement, usually composed of fibers, impart the required strength and stiffness to the composite material. Moreover, the fibers are surrounded by a polymer matrix, that enables the transmission of stresses and strains between the reinforcement and the support by in-plane shear as well as prevents the fibers to be spoiling.

Composite materials offer numerous advantages over traditional methods for strengthening and rehabilitating structures. These benefits include being lightweight, highly durable, and possessing impressive anti-corrosion properties [36]. Additionally, FRP materials offer unique mechanical properties that enable discrete as well as minimally intrusive strengthening and repair treatments toward structural elements. This is particularly important for historical, ancient, or architecturally important buildings where the structural elements cannot be easily replaced or rebuilt. The ability to incorporate FRP-based solutions into the original design of a building without impacting its aesthetic appeal allows for the seamless integration of architectural and structural requirements.

This study aims to examine the effectiveness of using a novel and flexible FRP material called Carbon-FRP (CFRP) ropes as a shear-strengthening system for rectangular RC beams. CFRP ropes are constructed using flexible unidirectional carbon fibers and have a lower unit price than CFRP strips. The study also compared the effectiveness of using CFRP ropes with steel bars as Near Surface Mounted (NSM) systems for shear strengthening. Additionally, the compressive zone of the beams, as illustrated in during earthquakes is important, and the usefulness of steel-reinforced geopolymer to enhance the flexural strength of the specimens within the compressive zone is also investigated. Fig. 1 illustrates the application of the strengthening method in both the real structure and

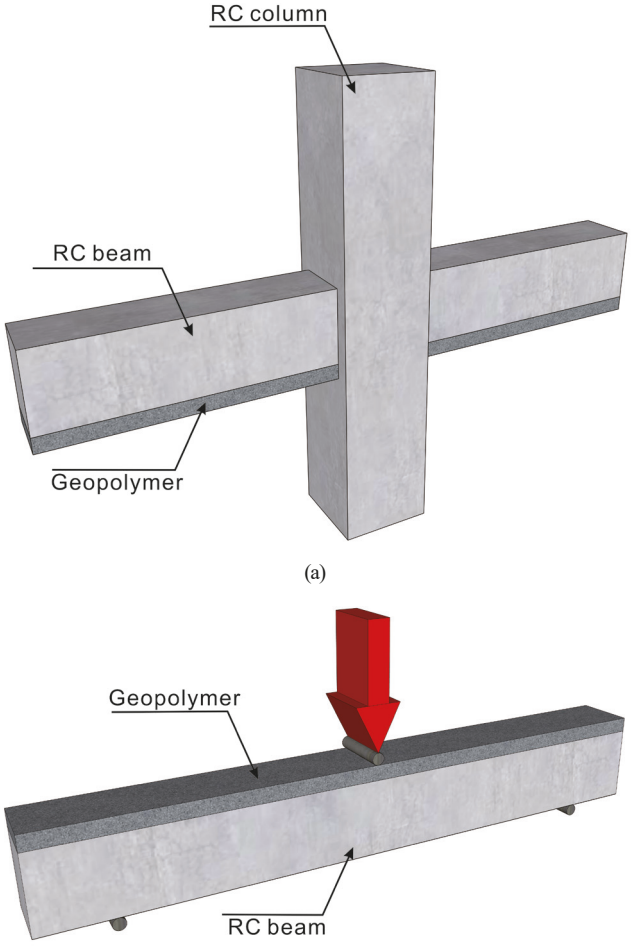

Fig. 1 The application of the strengthening method: (a) Real structure, (b) Experimental test

the experiment. Finally, a numerical model was developed to predict the ultimate load of the beams. The literature related to the utilization of NSM-CFRP ropes for shear strengthening of RC beams is limited, making this study a valuable contribution to the field.

2 Experimental program

2.1 Material

The geopolymer concrete was made from coarse aggregate, river sand, alkaline activators, and fly ash (FA) as industrial waste product. The mix proportion used is shown in Table 1. The alkaline activator (AA) used in the experiment was a mixture of 12 M sodium hydroxide (NaOH) solution and sodium silicate (Na_2SiO_3) in a ratio of Na_2SiO_3/NaOH solution of 2.5. NaOH dissolves aluminosilicate while Na_2SiO_3 acts as a binder, plasticizer, or dispersion in the presence of NaOH [37]. The adopted AA to FA ratio is 0.54. Ready-mixed normal-strength concrete was obtained from a local supplier, PT Sambas Wijaya Beton Concrete mixing plant. Three standard cylinders (∅150 mm × 300 mm) were used to determine the compressive strength of both geopolymer and normal concrete, following the ASTM C39/C39M-14 [38] standard. The results obtained were 27 MPa and 28 MPa, respectively.

The steel cages of all RC beam specimens were constructed using steel bars of three different diameters: 6 mm, 13 mm, and 19 mm. The longitudinal reinforcement of the RC beams was made up of deformed bars with diameters of 19 mm and 13 mm, while plain bars with a diameter of 6 mm were used as stirrups. Table 2 displays the ultimate and yield tensile strengths of both the longitudinal and transverse reinforcement.

Table 1 Mix the proportion of geopolymer

Raw materials	Composition
Aggregate: Binder (FA+AA)	70%:30%
Coarse aggregate: Fine aggregate	60%:40%
FA:AA	65%:35%
Na_2SiO_3:NaOH (12 M)	2.5:1.0
Extra water	11.70% × Binder (FA+AA)
Extra cement	5.63% × Binder (FA+AA)
Superplasticizer	2.00% × FA

Table 2 Mechanical properties of steel reinforcement

Bar diameter (mm)	Yield strength (MPa)	Ultimate strength (MPa)
19	473	633
13	334	461
6	328	439

The physical and mechanical properties of NSM-CFRP ropes and the adhesive are displayed in Tables 3 [39] and 4 [40], respectively. One specimen was treated with flexible NSM-CFRP ropes (SikaWrap® FX-50C) made by SIKA. The CFRP rope comprised a set of unidirectional carbon fibers bundled together and encased in a plastic envelope, which produced a new type of flexible NSM-CFRP material. To install the ropes, a groove was made in the significant range of the specimen, and Sika brand adhesive (Sikadur®-752) was used, with all properties supplied by the manufactory. The highest tensile load that the ropes could withstand before failure was determined to be 164 kN based on the total area of the FX ropes, which was 78 mm^2.

2.2 Beams specimens

In this study, a total of three rectangular RC beams were produced and examined. All RC beam specimens were constructed using ordinary ready-mix normal-strength concrete with a designed compressive strength of 25 MPa and had dimensions of 150 mm (width) × 330 mm (thickness) × 2500 mm (length). Among the three specimens, one was left un-strengthened as a control. The other

Table 3 Physical and mechanical properties of CFRP rope

Fiber type	NSM-CFRP
Weight	≥50 g/m (carbon fiber content)
Fiber cross-section	≥28 mm^2 (based on carbon fiber)
Fiber density	1.82 g/cm^2
Dry fiber properties in the longitudinal direction of the fibers	
Tensile modulus, minimum	2.4×10^5 MPa
Tensile strength, minimum	4000 MPa
Strain at break	≥0.016
Composite properties according to ASTM D4018-17 [39]	
Tensile modulus	2.3×10^5 MPa
Tensile strength	2000 MPa
Composite cross-section	64.526 mm^2

Table 4 Properties of SIKA epoxy adhesive (Sikadur®-752)

Information	Description
Color	Yellowish
Packaging	5 kg set
Density	1.08 kg/L
7 days compressive strength [40]	50–60 MPa
28 days compressive strength [40]	54–64 MPa
Modulus of elasticity in compression	1060 MPa
Tensile adhesion strength to concrete [40]	2 MPa
Tensile adhesion strength to steel [40]	9 MPa
Coefficient of thermal expansion	89×10^{-6} per °C

two were strengthened in shear with different materials, including NSM-steel bars and NSM-CFRP ropes, along with steel-reinforced geopolymer flexural strengthening, as shown in Fig. 2.

All the RC beam specimens were produced together using the same concrete mixture and then subjected to three-point bending tests until failure at the structures laboratory of Jenderal Soedirman University (UNSOED), Indonesia. The longitudinal reinforcement of the beams comprised two 13 mm diameter bottom bars and three 19 mm diameter top bars. Meanwhile, the shear reinforcement consisted of ∅6 mm stirrups with a spacing of 250 mm center to center. In the specimen IDs shown in Table 5, the second letter "N" and "G" indicate normal and geopolymer concrete, respectively. The third letter, "S" and "C", represent the two different types of materials (steel and CFRP) used for shear strengthening.

2.3 Testing setup

RC beams were arranged in a top-down position with a clear span of 2.2 m. A three-point bending system was employed to ensure that maximum bending and shear stress occurred

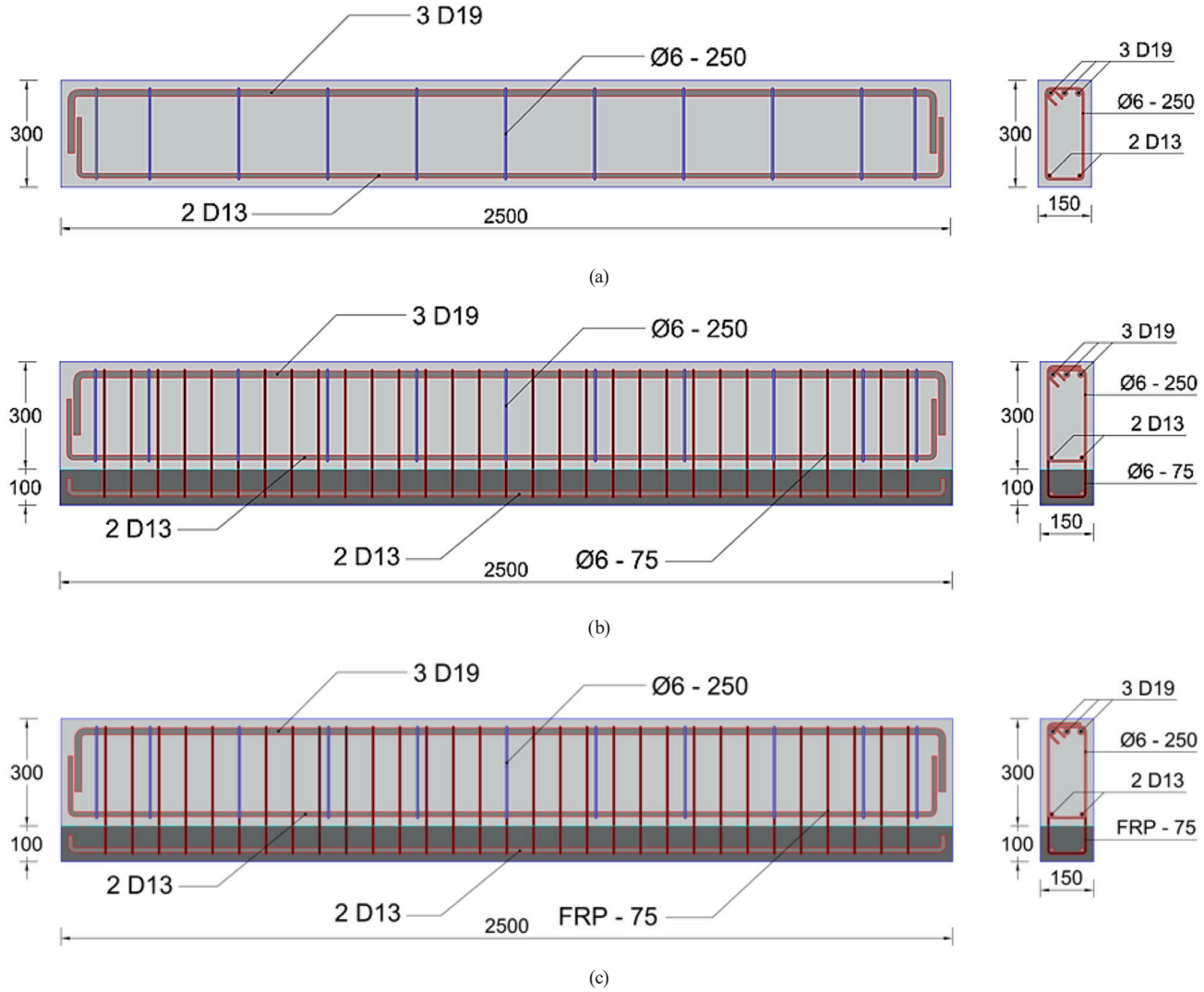

Fig. 2 Dimensions of beam specimens (unit: mm): (a) Specimen BN, (b) Specimen BGS, (c) Specimen BGC

Table 5 Specimen details

Specimen ID	Longitudinal reinforcement		Transverse reinforcement	Strengthening	
	Top	Bottom		Flexure	Shear
BN	3D19	2D13	∅6–250	–	–
BGS	3D19	2D13	∅6–250	Geopolymer	NSM-steel bars
BGC	3D19	2D13	∅6–250	Geopolymer	NSM-CFRP ropes

simultaneously at midspan, generating a compressive zone in the steel-reinforced geopolymer layer, as illustrated in Fig. 3. A hydraulic jack, with a load capacity of 500 kN, applied a vertical static load. This load was transferred to a rigid steel block connected to a steel rod fixed at the loading point. The beams were secured at both ends using steel plates and bolts to prevent any vertical translation while allowing horizontal movement to simulate simply supported conditions. To measure the vertical and horizontal displacements, four linear variable differential transformers (LVDTs) with an accuracy of ±0.01 mm were positioned as follows: two LVDTs were placed at midspan, one on each side of the beam to measure vertical displacement, and the other two were positioned at the quarter span on the left support to measure horizontal displacement. The load was incrementally increased at a controlled rate of 120 kN/s to avoid dynamic effects [41]. Cracks were visually monitored and marked on the side surfaces of the beams until failure occurred. A high-precision data logger was used to continuously record the load and displacement values.

3 Test results and discussion

3.1 Load-displacement responses

Fig. 4 displays the load-displacement curves for the control beam and the beams strengthened in shear with NSM-steel bars and NSM-CFRP ropes, both incorporating steel-reinforced geopolymer in the compression zone. Fig. 5 summarizes the crack, yield, and ultimate loads of all beam specimens. The strengthened beams exhibited significantly higher load capacity and displacement than the control beam. The combination of geopolymer concrete, steel bars, and CFRP ropes in the strengthening system improved the mechanical performance, allowing for the exploitation of steel bars in the post-yielding stage, thereby leading to higher load capacity. These results confirm those reported in previous studies [42, 43]. The load-displacement behaviors of the strengthened beams were nearly identical, indicating the similar significance of the two strengthening techniques.

The load-displacement curves of the beams exhibit a three-linear response that can be divided into three stages: elastic state, concrete cracking to steel yielding, and steel yielding to ultimate failure. All beams displayed linear and elastic behavior during the first stage due to excellent bonding between the materials before crack initiation. The second stage is characterized by the formation of cracks in the concrete section at the midpoint of the beams. The first cracking load for BGS and BGC was 28.91% and 50.87% higher, respectively, compared to the un-strengthened specimen. The flexural steel bars were theoretically yielded at about 75% of the ultimate load or 95.90 kN, 139.95 kN, and 147.34 kN for BN, BGS, and BGC specimens, respectively. In the third stage, the steel bars yield, and the strengthening materials held the crack width until beam failure. Specimens BGS and BGC showed an improvement of 45.78% and 53.49%, respectively, in the ultimate load compared to the control beam (BN).

3.2 Failure modes

Fig. 6 demonstrates the failure modes of the control beam and the beams strengthened in shear with different materials (NSM-steel bars and NSM-CFRP ropes) in combination with steel-reinforced geopolymer in the compression zone. The first cracking occurred close to the loading

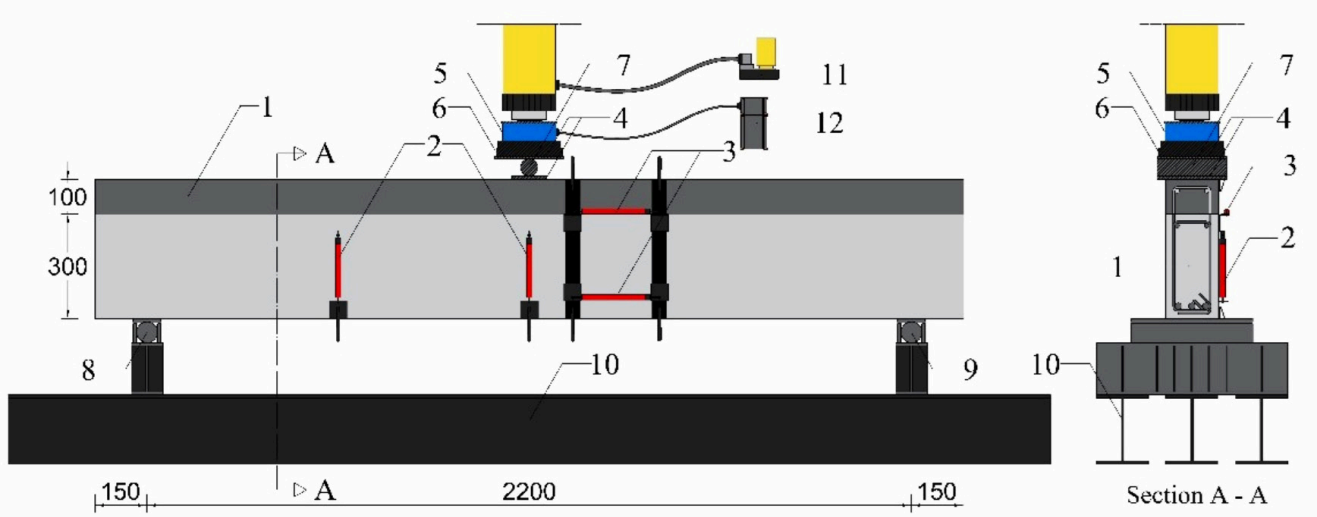

Fig. 3 Test setup (unit: mm): 1 – RC beams specimen, 2 – Vertical LVDTs, 3 – Horizontal LVDTs, 4 – Steel plate, 5 – Load cell, 6 – Steel block, 7 – Steel rod, 8 – Left support, 9 – Right support, 10 – Strong floor, 11 – Hydraulic jack, 12 – Data logger

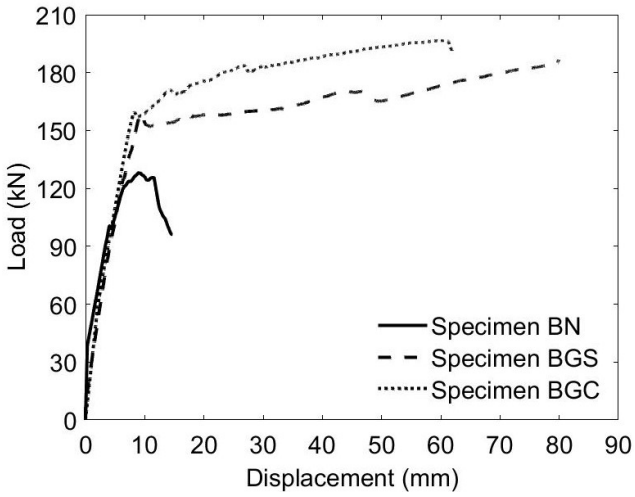

Fig. 4 Load-displacement curves of tested beams

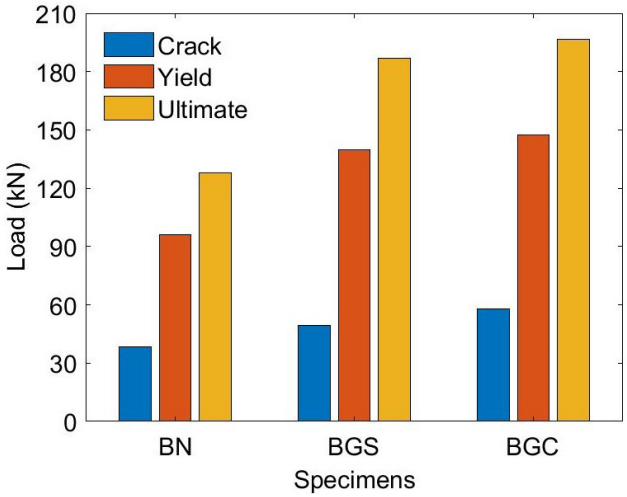

Fig. 5 Load summary of tested beams

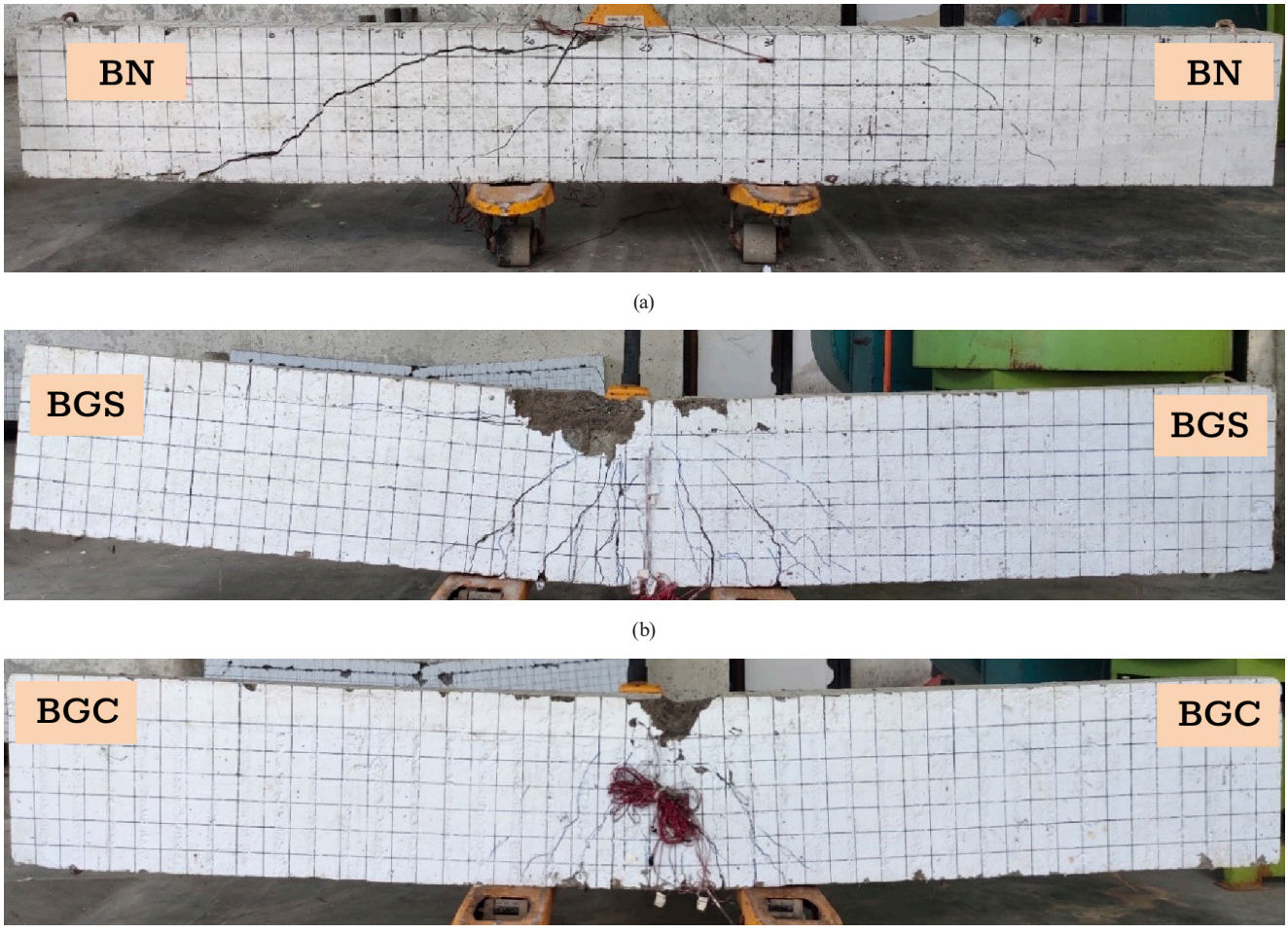

(a)

(b)

(c)

Fig. 6 Failure mode of control beam and strengthened beams: (a) Specimen BN, (b) Specimen BGS, (c) Specimen BGC

point in the control beam and mid-span in the strengthened beams, at loads of 38.38 kN, 49.48 kN, and 57.90 kN for BN, BGS, and BGC, respectively. Vertical cracks started to appear in the shear span as the load got higher, and these cracks eventually grew into critical diagonal ones that spread toward the loading points. The NSM-steel bars and NSM-CFRP ropes effectively hindered the development of shear cracks. The first crack in the strengthened beams, on the other hand, quickly expanded and spread through the compressive zone at the beam's top.

All specimens exhibited primary failure modes during the ultimate limit state test that were brought on by shear-tension (diagonal-tension) failure. After shear-tension cracks degraded the structures, two secondary failure types were found, which expedited the rupture of the beams. Shear-compression failure was the first secondary failure type, which developed from the crushing of concrete under the loading points caused by shear cracks across the prisms and limiting the shear-compression zone of the beams. This failure mode was predominantly discovered in strengthened beams. The second type, also observed in the strengthened beams, was flexural failure. The NSM-steel bars and NSM-CFRP ropes effectively suppressed the propagation of shear cracks.

As indicated in Fig. 6, splitting cracks between the existing concrete and geopolymer were discovered in the beam strengthened with NSM-steel bars (BGS). In contrast, similar cracks were not found in the NSM-CFRP rope-strengthened beam (BGC). By efficiently preventing the spread of shear cracks, NSM-steel bars and NSM-CFRP ropes greatly increased the ultimate strength of the strengthened beams (186.69 kN and 196.56 kN) in comparison to the control beam (128.06 kN).

3.3 Ductility performance

Ductility is the ability of RC beams to experience deformation exceeding the elastic limit while retaining an adequate load-carrying capacity until complete failure according to Pam et al. [44]. To guarantee the anticipated failure of the structural element, ductility is an essential design parameter that must be established [45]. The ratio between the displacements at peak load (δ_{max}) and the theoretical yield point of (δ_y) was used to quantitatively define the ductility. In this study, the yield point was determined using the equivalent elastoplastic system (bilinear approximation method), which involves identifying the point where the load-displacement curve deviates from linearity [46]. Table 6 displays the ductility indices of the examined specimens. The outcomes demonstrated that, depending on the material employed, the NSM approach enhanced the ductility of RC beams. The strengthened beams, in particular, demonstrated a considerable improvement in ductility, with a ratio of 2.61 and 2.19 for BGS and BGC, respectively, compared to the control beam. The improved ductile behavior of the strengthened beams can be attributed to the practical control of shear cracks by NSM-steel bars as well as NSM-CFRP ropes.

3.4 Stiffness

The stiffness values exhibited by test specimens can provide insight into the influence of strengthening materials. The stiffness values were computed in this study by determining the slopes of the lines connected to the load associated with the theoretical yield point. The use of NSM-steel bars and NSM-CFRP ropes for shear strengthening, along with the addition of steel-reinforced geopolymer in the compression zone, may not only have a positive impact on the RC beam in terms of increased strength and ductility, but may also play a role in reducing its stiffness, according to an analysis of the stiffness values. Table 7 shows the stiffness values for each specimen, indicating that the NSM-steel bars and NSM-CFRP ropes had opposing impacts on the stiffness of the strengthened beams. The NSM-steel bars approach, for example, generated a less favorable result in specimen BGS, moderately lowering stiffness by at least 29.88%. Similarly, specimen BGC strengthened with NSM-CFRP ropes exhibited a marginal stiffness reduction of 20.12% compared to the control beam. The lower stiffness values of the strengthened beams may be attributed to a higher degree of cracking, which is considered the most important factor affecting its stiffness.

3.5 Energy absorption capacity

The capacity of composites as repair material to absorb energy is of great importance, especially for structures that are exposed to dynamic loads, such as seismic, impact, or blast. The strengthening materials utilized in this study are well-suited for such applications. The capacity to absorb energy is closely related to the toughness of the material and its deflection-hardening behavior [47]. This was evaluated by calculating the area under the load-deflection curve. Fig. 7 indicates that the beams strengthened by NSM-steel bars and NSM-CFRP ropes had superior energy absorption capacity compared

Table 6 Ductility indices of tested beams

Specimen ID	δ_y (mm)	δ_{max} (mm)	Ductility index, δ_{max}/δ_y
BN	4.99	8.96	2.95
BGS	10.38	79.95	7.70
BGC	9.60	60.54	6.46

Table 7 Stiffness of tested beams

Specimen ID	δ_y (mm)	P_u (kN)	Stiffness, P_u/δ_y (kN/mm)
BN	4.99	128.06	25.64
BGS	10.38	186.69	17.98
BGC	9.60	196.56	20.48

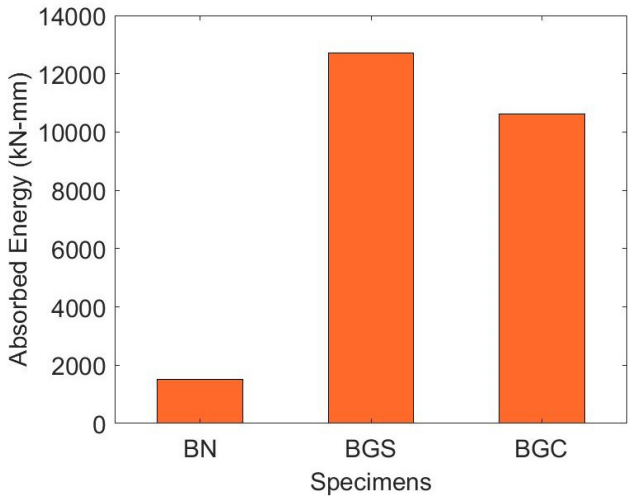

Fig. 7 Energy absorption capacity of tested beams

to the un-strengthened beam. For example, BGS was capable of absorbing energy up to 12704 kN-mm, presumed to be more than eight times greater than the control specimen. Similarly, using NSM-CFRP ropes (BGC) resulted in an approximately seven times increase in the absorption capacity at an energy level of 10629 kN-mm. The enhanced ability of the strengthened beams to absorb energy is primarily due to the excellent toughening effect of the strengthening materials.

4 Numerical approach

4.1 Model geometry

In order to accurately simulate the behavior of the tested beams, it was necessary to use plane elements to model the concrete and geopolymer. For this purpose, eight-node quadrilateral isoparametric Gauss integration solid elements (CQ16M) were utilized, with each node having two degrees of freedom in translational displacement variables along the X and Y directions. The longitudinal steel reinforcements, transverse shear stirrups, and CFRP ropes were modeled using automatically embedded reinforcement types and bars that could be embedded into all kinds of structural elements. This embedding concept means that reinforcement elements can automatically enter and couple with any surrounding mother elements without requiring the manual establishment of bond interface elements, thereby contributing to stiffness only through embedded reinforcement and mother elements. In order to avoid stress concentration during testing, steel plates with a thickness of 25 mm and the same width as the web of the beams were installed at the loading point and end support. These plates were simulated using CQ16M elements.

According to Zheng et al. [48], a numerical convergence study revealed that reducing the mesh size in the finite element analysis (FEA) had little impact on the numerical result but significantly increased the computation time. Therefore, to achieve the highest computational efficiency and reduce the run period, the largest global size of the elements used in the FEA was set to 25 mm. It is worth noting that all meshes were automatically generated by DIANA. Since the test conditions of the beams were symmetrical, its geometry was modeled with only half of its span in 2D plane-stress analysis, as shown in Fig. 8. In order to obtain the behavior of the specimens in the complete loading range, a displacement-controlled loading process was selected in the FEA. The vertical displacement was applied to the loading point using a rigid steel plate to prevent the occurrence of stress concentration.

4.2 Material models

The stress-strain constitutive relationship model of the materials is depicted in Fig. 9, where steel and CFRP are subject to axial strains and stresses via uniaxial constitutive laws. However, because concrete is heterogeneous, applying an evenly distributed external load to it may cause uneven internal stress and deformation distribution. As the external load increases, the material becomes weaker due to the progressive collapse of internal bonding between the mortar and aggregate caused by unevenly distributed internal strength and initial internal stress.

There are three different phases to the compressive stress-strain curve of plain concrete, each having its own

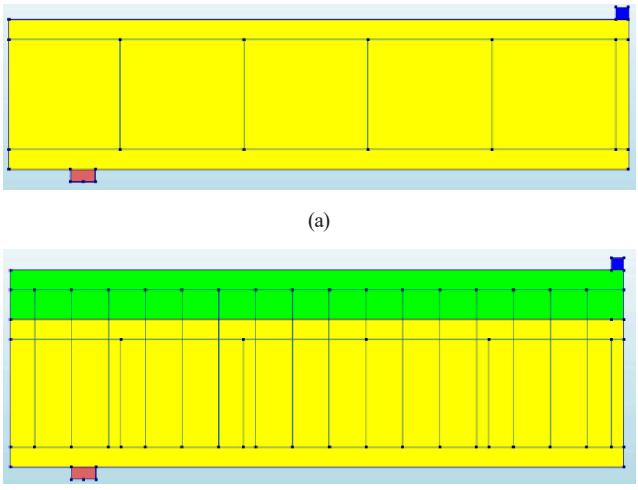

(a)

(b)

Fig. 8 Numerical model of beams: (a) Control beam, (b) Strengthened beam

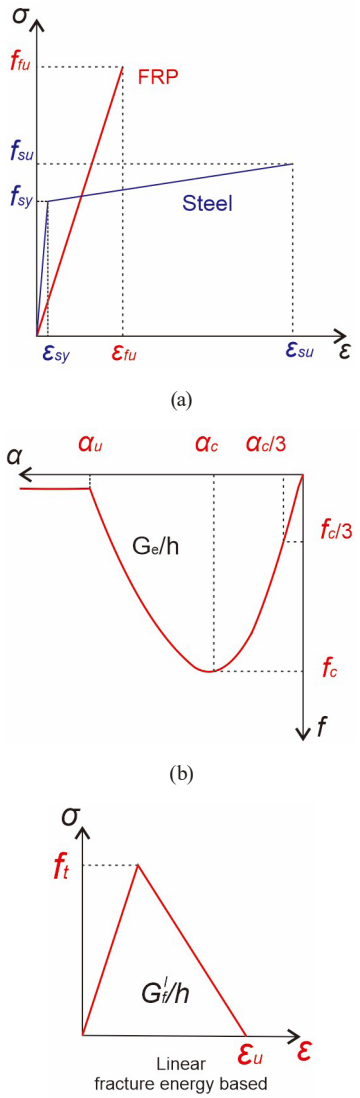

Fig. 9 Constitutive relationship model of the materials: (a) Steel reinforcement and CFRP, (b) Parabolic compression curve of concrete, (c) Tension softening curve of concrete

unique features. Concrete behaves linearly elastically at the first stage, which comprises 0% to 30% of the peak stress, and fracture growth is low. However, some preexisting bond cracks may already be present due to factors such as cement paste volume changes during hydration or drying shrinkage. In the second stage, which lasts from 70% to 90% of the peak stress, mortar cracks join neighboring bond cracks and new bond cracks start to emerge. In the third stage, the load is decreased to stop the uncontrolled spread of cracks as the stress level rises, the cracks continue to merge, and their growth becomes unstable.

The crack growth that occurs before the peak load is considered stable and only takes place when the load is increased. When a material or structure is subjected to a continual rise in deformation, it gradually loses its mechanical resistance, which is referred to as softening. As a result, softening starts happening in concrete during the post-peak lowering of mechanical resistance [49]. In order to accurately represent the physical behavior described in the preceding section, DIANA provides a number of concrete compression models. The parabolic compression curve is one such model, which is made up of four functions that change depending on the strain level. The curve follows the elastic modulus E_c in a straight line until it reaches one-third of the strain at maximum compressive strength (f_c).

That is, for $\alpha_c/3 < \alpha_j \leq 0$:

$$f = -f_c \frac{1}{3}\left(\frac{\alpha_j}{\frac{\alpha_c}{3}}\right). \tag{1}$$

When $\alpha_c < \alpha_j \leq \alpha_c/3$ the function takes the form:

$$f = -f_c \frac{1}{3}\left(1+4\left(\frac{\alpha_j-\frac{\alpha_c}{3}}{\alpha_c-\frac{\alpha_c}{3}}\right)-2\left(\frac{\alpha_j-\frac{\alpha_c}{3}}{\alpha_c-\frac{\alpha_c}{3}}\right)^2\right), \tag{2}$$

and for $\alpha_u < \alpha_j \leq \alpha_c$:

$$f = -f_c \frac{1}{3}\left(1+\left(\frac{\alpha_j-\alpha_c}{\alpha_u-\alpha_c}\right)^2\right). \tag{3}$$

When $\alpha_j \leq \alpha_u$ the function is either zero or a slight residual strength defined by the user, as displayed in Fig. 9 (a). The strain values are calculated using Eq. (4). As depicted in Fig. 9 (b), two variables influence the softening phase of the curve: the fracture energy, G, and the typical element length, h.

$$\frac{\alpha_c}{3} = -\frac{1}{3}\frac{f_c}{E};\ \alpha_c = \frac{5}{3}\frac{f_c}{E};\ \alpha_u = \min\left(\alpha_c - \frac{3}{2}\frac{G_c}{f_c'}2.5\alpha_c\right) \tag{4}$$

4.3 Model validation

Fig. 10 and Table 8 show the comparison between the experimental and numerical results. The finite element analysis (FEA) accurately predicted the load-displacement responses of the test beams at mid-span and loading point sections during different loading stages. The average value of the numerical loads ($P_{u\text{-}num}$) was 1.03, and the Normalized Mean Square Error (NMSE), as per Poli and Cirillo [50], was 3.55% when compared to the corresponding experimental loads ($P_{u\text{-}ex}$). In addition, the predicted maximum displacement ($\delta_{\max\text{-}num}$) had an average value and NMSE of 1.03 and 0.0001, respectively, compared

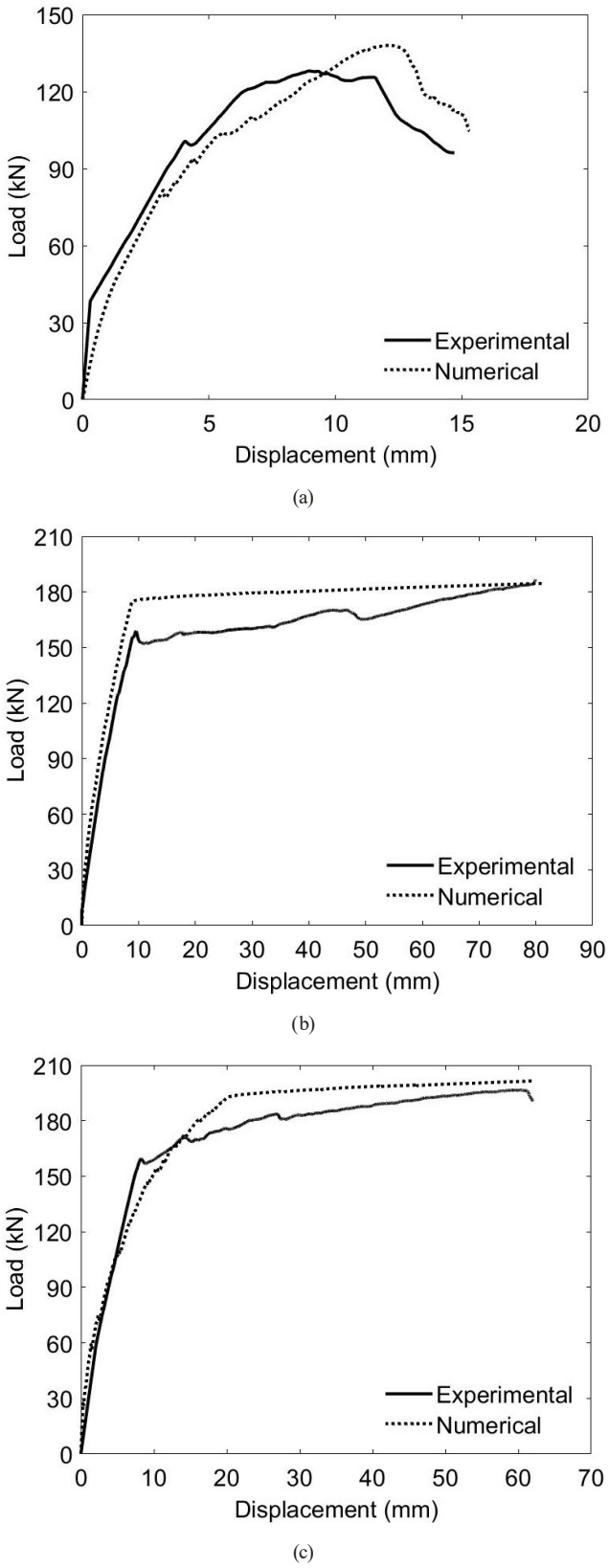

Fig. 10 Comparison between the experimental and numerical results: (a) Specimen BN, (b) Specimen BGS, (c) Specimen BGC

Table 8 Experimental and numerical results of the tested specimens

Specimen ID	Ultimate load (kN)		$P_{u\text{-}num}/P_{u\text{-}ex}$	Maximum displacement (mm)		$\delta_{max\text{-}num}/\delta_{max\text{-}ex}$
	$P_{u\text{-}ex}$	$P_{u\text{-}num}$		$\delta_{max\text{-}ex}$	$\delta_{max\text{-}num}$	
BN	128.06	138.05	1.08	14.71	15.31	1.04
BGS	186.69	184.61	0.99	79.96	80.99	1.01
BGC	196.56	201.53	1.03	60.54	62.12	1.03
Average			1.03			1.03
NMSE			0.0014			0.0001

to the test results ($\delta_{max\text{-}ex}$). The numerical results demonstrate that the FEA is capable of accurately predicting the load-displacement behavior of the beams strengthened in shear using NSM-steel bars and NSM-CFRP ropes, with the inclusion of steel-reinforced geopolymer in the compression zone. As a result, the numerical model functions as a dependable tool for making predictions, providing guidance for future design and experimental endeavors in the area of strengthening RC beams.

In addition, the FEA provided predicted results for certain parameters that could not be directly measured in the experiments, including the tensile equivalent plastic strains. Fig. 11 shows the comparison between the predicted and experimental tensile equivalent plastic strains for all the tested beams. The dimensions of tensile equivalent strains observed in the FEA are consistent with the concrete crack propagation observed in tested beams. The BGS and BGC strengthened beams demonstrated the highest tensile equivalent plastic strain in the tensile zone, which is situated between one-quarter and one-third of the total length. This finding suggests that the most significant flexural concrete crack occurs in this location because of stress concentration driven by the shift in cross-section. This phenomenon was also observed during the testing procedure.

5 Conclusions

This study investigated the behavior of RC beams strengthened in shear using the NSM technique, with the inclusion of steel-reinforced geopolymer in the compression zone. Three specimens were tested: two strengthened and one reference. The key parameters studied were NSM-steel bars and NSM-CFRP ropes. Based on a combination of experimental and numerical analyses, the significant findings are summarized as follows:

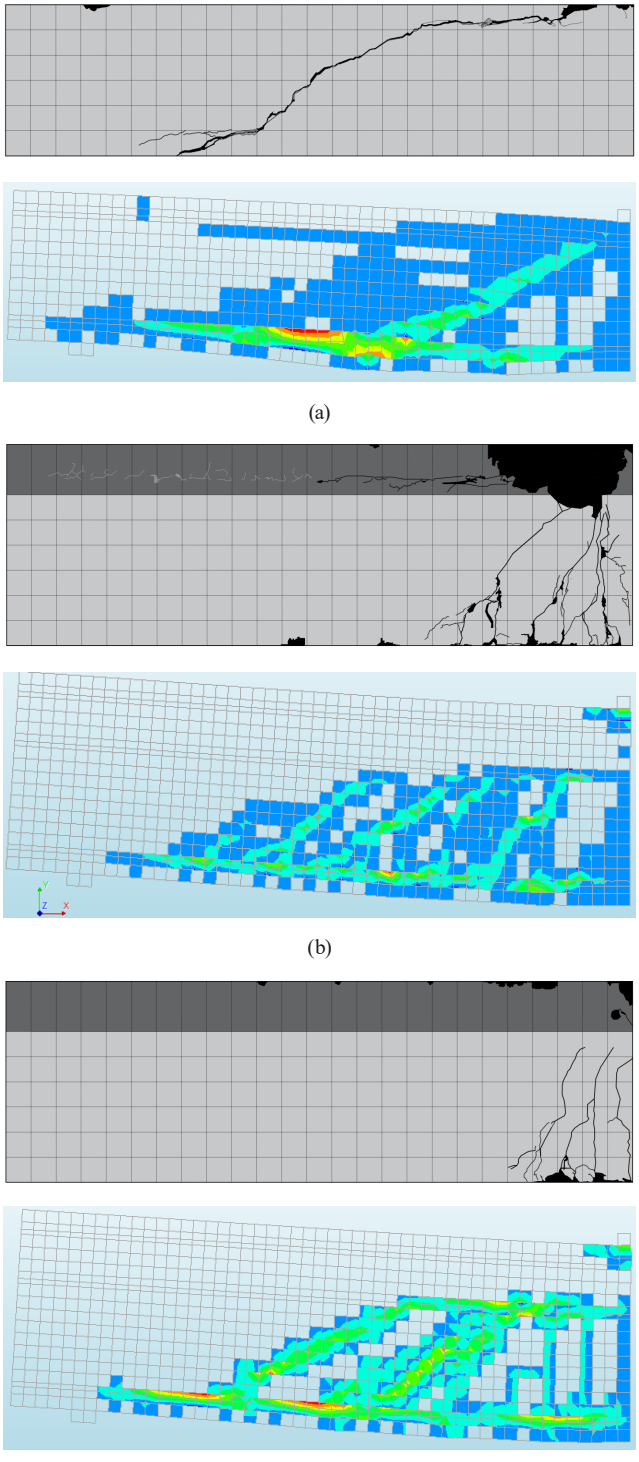

Fig. 11 Tensile equivalent plastic strains of the test beams: (a) Specimen BN, (b) Specimen BGS, (c) Specimen BGC

- The load-carrying capacity of the specimens strengthened with NSM-steel bars and NSM-CFRP ropes increased by factors of 1.46 and 1.53, respectively, compared to the reference specimen.
- The application of NSM-steel bars and NSM-CFRP ropes as shear strengthening techniques effectively delayed and prevented the propagation of shear cracks, resulting in enhanced capacity, ductility, and a significant increase in maximum deflection compared to the control beam.
- The strengthening method employed had a dual effect on the specimens: while it increased strength and ductility, it also reduced stiffness by approximately 30%.
- The beams strengthened with NSM-steel bars and NSM-CFRP ropes exhibited superior energy absorption performance compared to the control beam.
- The FEA results showed good agreement with the experimental data, demonstrating that the developed numerical model can accurately simulate the response of the tested specimens. This validates the numerical model as a reliable predictive tool, guiding future design and experimental efforts in the field of RC beam strengthening.

Acknowledgement

The gratitude is delivered by the authors to the Directorate General of Higher Education, the Ministry of Education and Culture of Indonesia (Dirjen Dikti), for supporting this study via the BPP-DN Scholarship, and Rendi Ariefta who provide assistances that this study is well accomplished.

References

[1] Hidayat, B. A., Hu, H.-T., Han, A. L., Haryanto, Y., Widyaningrum, A., Pamudji, G. "Nonlinear finite element analysis of traditional flexural strengthening using betung bamboo (*Dendrocalamus asper*) on concrete beams", In: 7th International Conference on Euro Asia, Stuttgart, Germany, 2019, 615, 012073. https://doi.org/10.1088/1757-899X/615/1/012073

[2] Haryanto, Y., Han, A. L., Hu, H.-T., Hsiao, F.-P., Hidayat, B. A., Widyaningrum, A. "Enhancement of flexural performance of RC beams with steel wire rope by external strengthening technique", Journal of the Chinese Institute of Engineers, 44(3), pp. 193–203, 2021. https://doi.org/10.1080/02533839.2021.1871651

[3] Haryanto, Y., Hu, H.-T., Han, A. L., Hsiao, F.-P., Wariyatno, N. G., Hidayat, B. A. "Numerical parametric study on the flexural capacity of reinforced concrete beams strengthened with non-metallic materials", Journal of Engineering Science and Technology, 16(4), pp. 3295–3311, 2021.

[4] Haryanto, Y., Hsiao, F.-P., Hu, H.-T., Han, A. L., Hidayat, B. A., Nugroho, L. "Validating an analytical method to predict flexural behavior of RC T-beams retrofitted with bonded steel wire ropes in the negative moment region", In: The 3rd International Conference on Engineering, Technology and Innovative Researches, Purbalingga, Indonesia, 2023, 2482(1), 030001. https://doi.org/10.1063/5.0113554

[5] Madotto, R., Van Engelen, N. C., Das, S., Russo, G., Pauletta, M. "Shear and flexural strengthening of RC beams using BFRP fabrics", Engineering Structures, 229, 111606, 2021. https://doi.org/10.1016/j.engstruct.2020.111606

[6] Pribadi, K. S., Abduh, M., Wirahadikusumah, R. D., Hanifa, N. R., Irsyam, M., Kusumaningrum, P., Puri, E. "Learning from past earthquake disasters: The need for knowledge management system to enhance infrastructure resilience in Indonesia", International Journal of Disaster Risk Reduction, 64, 102424, 2021. https://doi.org/10.1016/j.ijdrr.2021.102424

[7] Haryanto, Y., Gan, B. S., Maryoto, A. "Wire rope flexural bonded strengthening system on RC-beams: a finite element simulation", International Journal of Technology, 8(1), pp. 134–144, 2017. https://doi.org/10.14716/ijtech.v8i1.2734

[8] Haryanto, Y., Gan, B. S., Widyaningrum, A., Maryoto A. "Near surface mounted bamboo reinforcement for flexural strengthening of reinforced concrete beams", Jurnal Teknologi, 79(6), pp. 233–240, 2017. https://doi.org/10.11113/jt.v79.10767

[9] Haryanto, Y., Gan, B. S., Widyaningrum, A., Wariyatno, N. G., Fadli, A. "On the performance of steel wire rope as the external strengthening of RC beams with different end-anchor type", Jurnal Teknologi, 80(5), pp. 145–154, 2018. https://doi.org/10.11113/jt.v80.11588

[10] Haryanto, Y., Hu, H.-T., Lie, H. A., Atmajayanti, A. T., Galuh, D. L. C., Hidayat, B. A. "Finite element analysis of T-Section RC beams strengthened by wire rope in the negative moment region with an addition of steel rebar at the compression block", Jurnal Teknologi, 81(4), pp. 143–154, 2019. https://doi.org/10.11113/jt.v81.12974

[11] Ferrotto, M. F., Cavaleri, L., Papia, M. "Compressive response of substandard steel-jacketed RC columns strengthened under sustained service loads: From the local to the global behavior", Construction and Building Materials, 179, pp. 500–511, 2018. https://doi.org/10.1016/j.conbuildmat.2018.05.247

[12] Salah, A., Elsanadedy, H., Abbas, H., Almusallam, T., Al-Salloum, Y. "Behavior of axially loaded L-shaped RC columns strengthened using steel jacketing", Journal of Building Engineering, 47, 103870, 2022. https://doi.org/10.1016/j.jobe.2021.103870

[13] Ibrahim, A. M. A., Diab, H. M., Hassanean, Y. A., Farghal, O. A., Ismail, M. M. A. "Numerical study on the behavior and strength of concrete beam strengthening with fiber reinforced concrete jackets", Structures, 50, pp. 1557–1572, 2023. https://doi.org/10.1016/j.istruc.2023.02.112

[14] Aldahdooh, M. A. A., Muhammad Bunnori, N., Megat Johari, M. A., Jamrah, A., Alnuaimi, A. "Retrofitting of damaged reinforced concrete beams with a new green cementitious composites material", Composite Structures, 142, pp. 27–34, 2016. https://doi.org/10.1016/j.compstruct.2016.01.067

[15] Peng, G., Niu, D., Hu, X., Zhong, S., Huang, D. "Experimental and theoretical study on the flexural behavior of RC beams strengthened with cementitious grout", Engineering Structures, 267, 114713, 2022. https://doi.org/10.1016/j.engstruct.2022.114713

[16] Peng, G., Hu, X., Niu, D., Zhong, S., Huang, D. "Experimental study on the shear behavior of RC beams strengthened with cementitious grout", Structures, 50, pp. 1403–1415, 2023. https://doi.org/10.1016/j.istruc.2023.02.115

[17] Zanotti, C., Borges, P. H. R., Bhutta, A., Banthia, N. "Bond strength between concrete substrate and metakaolin geopolymer repair mortar: Effect of curing regime and PVA fiber reinforcement", Cement and Concrete Composites, 80, pp. 307–316, 2017. https://doi.org/10.1016/j.cemconcomp.2016.12.014

[18] Ahmad Zailani, W. W., Bouaissi, A., Abdullah, M. M. A. B., Abd Razak, R., Yoriya, S., Mohd Salleh, M. A. A., Rozainy, M. A Z. M. R., Fansuri, H. "Bonding Strength Characteristics of FA-Based Geopolymer Paste as a Repair Material When Applied on OPC Substrate ", Applied Sciences, 10(9), 3321, 2020. https://doi.org/10.3390/app10093321

[19] Ricciotti, L., Molino, A. J., Roviello, V., Cennamo, P., Chianese, E., Roviello, G. "Geopolymer Composites for Potential Applications in Cultural Heritage", Environments, 4(4), 91, 2017. https://doi.org/10.3390/environments4040091

[20] Pacheco-Torgal, F., Abdollahnejad, Z., Miraldo, S., Baklouti, S., Ding, Y. "An overview on the potential of geopolymers for concrete infrastructure rehabilitation", Construction and Building Materials, 36, pp. 1053–1058, 2012. https://doi.org/10.1016/j.conbuildmat.2012.07.003

[21] Haryanto, Y., Hu, H.-T., Han, A. L., Hsiao, F.-P., Teng, C.-J., Hidayat, B. A., Nugroho, L. "Nonlinear 3D Model of Double Shear Lap Tests for the Bond of Near-surface Mounted FRP Rods in Concrete Considering Different Embedment Depth", Periodica Polytechnica Civil Engineering, 65(3), pp. 878–889, 2021. https://doi.org/10.3311/PPci.17309

[22] Haryanto, Y., Hu, H.-T., Han, A. L., Hsiao, F.-P., Teng, C.-J., Hidayat, B. A., Nugroho, L. "Numerical investigation on RC T-beams strengthened in the negative moment region using NSM FRP rods at various depth of embedment", Computers and Concrete, 28(4), pp. 347–360, 2021. https://doi.org/10.12989/cac.2021.28.4.347

[23] Haryanto, Y., Hu, H.-T., Han, A. L., Hsiao, F.-P., Teng, C.-J., Hidayat, B. A., Wariyatno N. G. "Negative moment region flexural strengthening system of RC T-beams with half-embedded NSM FRP rods: a parametric analytical approach", Journal of the Chinese Institute of Engineers, 44(6), pp. 553–561, 2021. https://doi.org/10.1080/02533839.2021.1936646

[24] Han, A. L., Hu, H.-T., Gan, B. S., Hsiao, F.-P., Haryanto, Y. "Carbon Fiber-Reinforced Polymer Rod Embedment Depth Influence on Concrete Strengthening", Arabian Journal for Science and Engineering, 47(10), pp. 12685–12695, 2022. https://doi.org/10.1007/s13369-022-06601-2

[25] Haryanto, Y., Hsiao, F.-P., Hu, H.-T., Han, A. L., Chua, A. W., Salim, F., Nugroho, L. "Structural behavior of negative moment region NSM-CFRP strengthened RC *T*-beams with various embedment depth under monotonic and cyclic loading", Composite Structures, 301, 116214, 2022.
https://doi.org/10.1016/j.compstruct.2022.116214

[26] Haryanto, Y., Han, A. L., Hu, H.-T., Hsiao, F.-P., Gan, B. S., Nugroho, L., Lin, C.-C. "Impact of Non-Reversed Low Cyclic Loading on the Seismic Response of RC T-Beams Strengthened in the Hogging Zone Using NSM-CFRP Rods with Different Embedment Depth", In: The 33rd International Ocean and Polar Engineering Conference, Ottawa, Canada, 2023, pp. 3191–3201. ISBN 978-1-880653-80-7

[27] Haryanto, Y., Hermanto, N. I. S., Hsiao, F.-P., Hu, H.-T., Han, A. L., Nugroho, L., Fernando, S. "Predicting the behavior of RC T-beams strengthened with NSM-CFRP rods in the negative moment region: A finite element approach for low cyclic loading", In: The 2nd International Conference on Disaster Mitigation and Management, Padang, Indonesia, 2023, 464, 06001. ISBN 9781713886563
https://doi.org/10.1051/e3sconf/202346406001

[28] Nugroho, L., Haryanto, Y., Hu, H.-T., Hsiao, F.-P., Han, A. L., Widyaningrum, A., Prasetijo, H. "Flexural capacity of negative moment region NSM-CFRP strengthened RC T-beam under high loading rate: An analytical prediction", In: The 2nd International Conference on Disaster Mitigation and Management, Padang, Indonesia, 2023, 464, 06004. ISBN 9781713886563
https://doi.org/10.1051/e3sconf/202346406004

[29] Nugroho, L., Haryanto, Y., Hu, H.-T., Han, A. L., Hsiao, F.-P., Lin, C.-C., Weng, P.-W., Widiastuti, E. P. "NSM-CFRP rods with varied embedment depths for strengthening RC T-beams in the negative moment region: Investigation on high cyclic response", Composite Structures, 331, 117891, 2024.
https://doi.org/10.1016/j.compstruct.2024.117891

[30] Tafsirojjaman, T., Dogar, A. U. R., Liu, Y., Manalo, A., Thambiratnam, D. P. "Performance and design of steel structures reinforced with FRP composites: A state-of-the-art review", Engineering Failure Analysis, 138, 106371, 2022.
https://doi.org/10.1016/j.engfailanal.2022.106371

[31] Daouadji, T. H., Abderezak, R., Rabia, B. "New technique for repairing circular steel beams by FRP plate", Advanced in Materials Research, 11(3), pp. 171–190, 2022.
https://doi.org/10.12989/amr.2022.11.3.171

[32] Huang, S., Yan, L., Kasal, B. "Flexural behaviour of wood beams strengthened by flax-glass hybrid FRP subjected to hygrothermal and weathering exposures", Construction and Building Materials, 365, 130076, 2023.
https://doi.org/10.1016/j.conbuildmat.2022.130076

[33] Lee, M.-G., Huang, Y., Kan, Y.-C., Wang, Y.-C., Chen, Y.-S., Kao, S.-C. "Experimental study on durability of CFRP-strengthened wood members", Journal of Materials Research and Technology, 24, pp. 3704–3716, 2023.
https://doi.org/10.1016/j.jmrt.2023.04.030

[34] D'Altri, A. M., de Miranda, S. "Environmentally-induced loss of performance in FRP strengthening systems bonded to full-scale masonry structures", Construction and Building Materials, 249, 118757, 2020.
https://doi.org/10.1016/j.conbuildmat.2020.118757

[35] Napoli, A., Realfonzo, R. "FRP confined masonry under compression: database collection and design proposals", Composite Structures, 276, 114490, 2021.
https://doi.org/10.1016/j.compstruct.2021.114490

[36] Yoshitake, I., Hasegawa, H., Shimose, K. "Monotonic and cyclic loading tests of reinforced concrete beam strengthened with bond-improved carbon fiber reinforced polymer (CFRP) rods of ultra-high modulus", Engineering Structures, 206, 110175, 2020.
https://doi.org/10.1016/j.engstruct.2020.110175

[37] Memon, F. A., Nuruddin, M. F., Khan, S., Shafiq, N., Ayub, T. "Effect of sodium hydroxide concentration on fresh properties and compressive strength of self-compacting geopolymer concrete", Journal of Engineering Science and Technology, 8(1), pp. 44–56, 2013.

[38] ASTM "ASTM C39/C39M-14 Standard Test Method for Compressive Strength of Cylindrical Concrete Specimens", American Society for Testing and Materials, West Conshohocken, PA, USA, 2014.
https://doi.org/10.1520/C0039_C0039M-14

[39] ASTM "ASTM D4018-17 Standard Test Methods for Properties of Continuous Filament Carbon and Graphite Fiber Tows", American Society for Testing and Materials, West Conshohocken, PA, USA, 2017.
https://doi.org/10.1520/D4018-17

[40] ASTM "ASTM D695-15 Standard Test Method for, Compressive Properties of Rigid Plastics", American Society for Testing and Materials, West Conshohocken, PA, USA, 2015.
https://doi.org/10.1520/D0695-15

[41] Tudjono, S., Han, A. L., Gan, B. S. "An Integrated System for Enhancing Flexural Members' Capacity via Combinations of the Fiber Reinforced Plastic Use, Retrofitting, and Surface Treatment Techniques", International Journal of Technology, 9(1), pp. 5–15, 2018.
https://doi.org/10.14716/ijtech.v9i1.298

[42] Saadah, M., Ashteyat, A., Murad, Y. "Shear strengthening of RC beams using side near surface mounted CFRP ropes and strips", Structures, 32, pp. 380–390, 2021.
https://doi.org/10.1016/j.istruc.2021.03.038

[43] Peng, K.-D., Huang, B.-T., Xu, L.-Y., Hu, R.-L., Dai, J.-G. "Flexural strengthening of reinforced concrete beams using geopolymer-bonded small-diameter CFRP bars", Engineering Structures, 256, 113992, 2022.
https://doi.org/10.1016/j.engstruct.2022.113992

[44] Pam, H. J., Kwan, A. K. H., Islam, M. S. "Flexural strength and ductility of reinforced normal- and high-strength concrete beams", Structures and Buildings, 146(4), pp. 381–389, 2001.
https://doi.org/10.1680/stbu.2001.146.4.381

[45] Guades, E. J., Stang, H., Schmidt, J. W., Fischer, G. "Flexural behavior of hybrid fibre-reinforced geopolymer composites (FRGC)-jacketed RC beams", Engineering Structures, 235, 112053, 2021.
https://doi.org/10.1016/j.engstruct.2021.112053

[46] Pamudji, G., Haryanto, Y., Hu, H.-T., Asriani, F., Nugroho, L. "The flexural behavior of RC beams with sand-coated polypropylene waste coarse aggregate at different w/c ratios", Advanced Materials Research, 10(4), pp. 313–329, 2021.
https://doi.org/10.12989/amr.2021.10.4.313

[47] Nematollahi, B., Sanjayan, J., Shaikh, F. U. A. "Comparative deflection hardening behavior of short fiber reinforced geopolymer composites", Construction and Building Materials, 70, pp. 54–64, 2014. https://doi.org/10.1016/j.conbuildmat.2014.07.085

[48] Zheng, Y.-Z., Wang, W.-W., Mosalam, K. M., Fang, Q., Chen, L., Zhu, Z.-F. "Experimental investigation and numerical analysis of RC beams shear strengthened with FRP/ECC composite layer", Composite Structures, 246, 112436, 2020. https://doi.org/10.1016/j.compstruct.2020.112436

[49] Vonk, T. A. "Softening of Concrete Loaded in Compression", PhD Thesis, Technische Universiteit Eindhoven, Eindhoven, The Netherlands, 1992. https://doi.org/10.6100/IR375705

[50] Poli, A. A., Cirillo, M. C. "On the use of the normalized mean square error in evaluating dispersion model performance", Atmospheric Environment. Part A. General Topics, 27(15), pp. 2427–2434, 1993. https://doi.org/10.1016/0960-1686(93)90410-Z